

## High-Precision X-Ray Polarimetry

B. Marx,<sup>1,\*</sup> K. S. Schulze,<sup>1,2</sup> I. Uschmann,<sup>1,2</sup> T. Kämpfer,<sup>1,2</sup> R. Löttsch,<sup>1,2</sup> O. Wehrhan,<sup>1,2</sup> W. Wagner,<sup>3</sup> C. Detlefs,<sup>4</sup>  
T. Roth,<sup>4</sup> J. Härtwig,<sup>4</sup> E. Förster,<sup>1,2</sup> T. Stöhlker,<sup>2</sup> and G. G. Paulus<sup>1,2</sup>

<sup>1</sup>*Institut für Optik und Quantenelektronik, Friedrich-Schiller-Universität Jena, Max-Wien-Platz 1, D-07743 Jena, Germany*

<sup>2</sup>*Helmholtz-Institut Jena, Helmholtzweg 4, D-07743 Jena, Germany*

<sup>3</sup>*Helmholtz-Zentrum Dresden-Rossendorf, Bautzner Landstraße 400, D-01328 Dresden, Germany*

<sup>4</sup>*European Synchrotron Radiation Facility, B. P. 220, F-38043 Grenoble Cedex, France*

(Received 28 January 2012; published 21 June 2013)

The polarization purity of 6.457- and 12.914-keV x rays has been improved to the level of  $2.4 \times 10^{-10}$  and  $5.7 \times 10^{-10}$ . The polarizers are channel-cut silicon crystals using six  $90^\circ$  reflections. Their performance and possible applications are demonstrated in the measurement of the optical activity of a sucrose solution.

DOI: [10.1103/PhysRevLett.110.254801](https://doi.org/10.1103/PhysRevLett.110.254801)

PACS numbers: 41.50.+h, 33.55.+b, 42.79.Ci

Polarimetry is one of the most versatile and sensitive methods in optics. Ellipsometry, e.g., reaches sensitivities down to a single atomic layer. Other applications include modulators in photonics, fluorescence polarization in chemistry, and scanning laser polarimetry in medicine. X-ray polarimetry, in contrast, has progressed more gradually even though the discovery of the polarization of x rays [1] predates the confirmation of their electromagnetic nature. Nevertheless, there are efficient methods for x-ray polarimetry [2–4] providing the basis for a few important applications, most notably in solid-state physics, see, e.g., Refs. [5,6]. In this Letter we report on the development and test of crystal polarimeters based on  $45^\circ$  Bragg diffraction. The polarization purity achieved reaches  $2.4 \times 10^{-10}$ . The corresponding extreme sensitivity is demonstrated by implementing a classic polarimetry experiment, the optical activity of sugar, in the x-ray spectral region.

The polarization purity  $P$  of x rays diffracted by a crystal is defined as the ratio of the intensity of the  $\pi$ - and  $\sigma$ -polarized component, both integrated over a certain angular and energy range around the Bragg angle and energy.  $\pi$  and  $\sigma$  denote the two directions of polarization, respectively parallel and normal to the scattering plane. With respect to a crossed-polarizer setup,  $P$  is the ratio of the transmitted flux in the perpendicular (“crossed”) and parallel position of the scattering planes, again integrated over angle and energy.

The first high-purity x-ray polarizers were developed for nuclear resonant scattering [7] where the tiny fraction of scattered x rays has to be discriminated against a large background of transmitted x rays. Due to the, in general, different polarization state of reemitted photons, this is possible if a sufficient purity of polarization is available. So far, scientists have used channel-cut crystals with two asymmetric reflections. A suppression of the  $\pi$  component by a factor of  $4 \times 10^{-8}$  was achieved in the best case [8]. Using four symmetric reflections, we recently achieved polarization purities in the order of  $10^{-9}$  [9].

Our efforts to further improve the properties of x-ray polarimeters were originally motivated by the pending evidence of birefringence of vacuum polarized by strong electric or magnetic fields. This effect, which was already predicted in the early days of quantum electrodynamics [10], has escaped detection so far due to its weakness. Estimations suggest a required polarization purity in excess of  $10^{-11}$  at wavelengths below 1 Å [11]. An interesting aspect of vacuum birefringence is its discovery potential for hypothetical new elementary particles [12,13]. Much more immediate for the high-definition polarizer may be novel applications emerging from an improvement of x-ray polarimetry by several orders of magnitude. Examples are x-ray quantum optics [14] and new opportunities in the field of nuclear resonant scattering because a delayed detection of the fluorescence can be avoided [15].

At x-ray photon energies of the order of 10 keV, the highest polarization purities can be achieved by reflection at perfect crystals at a Bragg angle of  $45^\circ$ . The incident and reflected beam will then enclose  $90^\circ$  and, as a consequence, the reflection coefficient for the  $\pi$  component will be identically zero. The condition of  $45^\circ$  Bragg reflection implies that any given crystal can only serve as a polarizer for a discrete set of narrow bands of wavelengths determined by the lattice planes of the respective crystal. Therefore, an energy bandwidth of about 1 eV and an incoming beam divergence in the range of the full width at half maximum of the rocking curve should not be exceeded.

Perfect polarization based on crystal diffraction demands a perfect crystal lattice. This requirement has to be fulfilled in particular within the penetration depth, i.e., close to the crystal surface which has to be prepared very carefully for this reason. Another major effect compromising the polarization purity is the multiple-beam case, where more than two reciprocal lattice points lie in the vicinity of the Ewald sphere. As a consequence, the incident beam not only excites the desired primary reflection with  $\theta_B = 45^\circ$ , but also a secondary reflection which in

turn can diffract in the direction of the primary reflection via a detour. The latter reflections are regularly not  $45^\circ$  reflections. Accordingly, they will have a nonvanishing reflection coefficient for the  $\pi$  component resulting in degraded polarization purity.

On the other hand, the purity can be increased by using a series of  $45^\circ$  reflections [16,17]. The most convenient way to realize this is to cut a trench into a crystal parallel to the desired lattice plane. Then the x-ray beam can be reflected at the walls of the trench as often as desired or the quality of the crystal permits. Such crystals are known as channel-cut crystals.

The intensity of multiple-beam effects is proportional to the cube of the atomic number of the element the channel cut is made of [18]. Therefore, the first measure to minimize polarization impurities is the selection of a suitable crystal. Silicon with an atomic number of just 14 is an attractive choice because highly perfect crystals with minimum impurities are readily obtainable and can easily be worked on.

Besides the selection of the right crystal, the preparation of the channel cuts requires sophisticated procedures. First of all, the channel has to be cut in such an orientation that multiple-beam cases are suppressed. The degree of freedom that can be exploited is a rotation around the normal of the reflection lattice planes, because this does not change the Bragg angle. In fact, each lattice plane may diffract all incident waves with wave vectors lying on a (Kossel) cone with an opening angle equal to twice the Bragg angle. Our strategy is to stay in the two-beam case and to avoid the excitation of any further beams. For this purpose, a computer code (“AZIMUTH”) has been developed to calculate all crystal reflections for a certain x-ray energy. The entire reflection system for a silicon crystal and an x-ray energy of 12.914 keV is displayed in Fig. 1. Each colored line represents the intersection of a Kossel cone with a virtual sphere around the crystal. Crossings of two or more of these lines indicate unwanted multiple-beam cases. The number of possible multiple-beam cases increases for shorter wavelengths because the radius of the Ewald sphere increases. Accordingly, more and more reciprocal lattice points may be close to it, which means that one has to expect that the polarization purity decreases.

As a result of the described optimization procedure, we choose for our measurements two different crystal azimuth orientations for different x-ray energies: Si(400) at 6.457 keV and Si(800) at 12.914 keV. After the orientation of the crystal, a careful preparation of the crystal surfaces has to be performed in order to suppress the intensity in the tails of the rocking curve which could excite multiple beam effects. The use of low-damage saw blades and different etching methods was found to be essential. The combination of a series of reflections in the channel cut, thoughtful crystal alignment, and careful surface preparation is decisive for achieving polarization purities of the order of  $10^{-10}$ .

The schematic setup of the x-ray polarimeter is shown in Fig. 2. Our measurements of polarization purities have

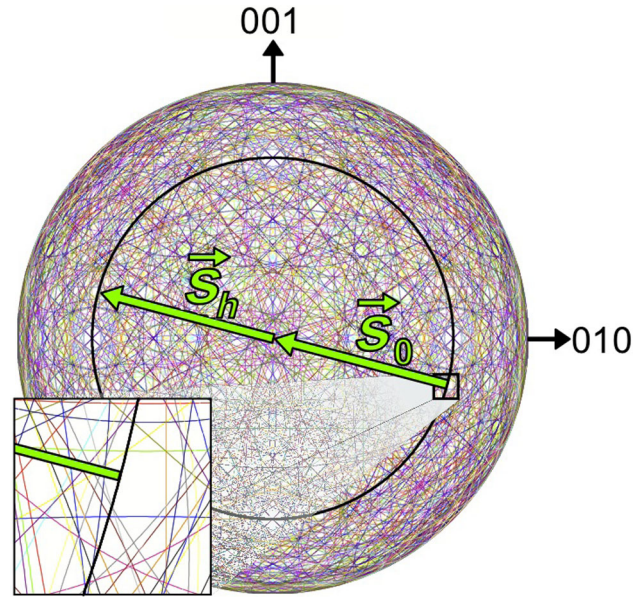


FIG. 1 (color online). Kossel pattern of silicon at 12.914 keV. The bold black circle represents the exploited Si (800) reflection used for suppression of the  $\pi$  component. All other possible reflections are depicted by thin colored circles. The vectors  $\vec{s}_0$  and  $\vec{s}_h$  describe the direction of the incident and diffracted wave respectively. In order to avoid degradation of the polarization purity due to multiple-beam cases, the azimuth has to be chosen such that the “distance” to the closest undesired reflections is as large as possible.

been carried out at the Techniques and Instrumentation Test beam line, ID06, of the European Synchrotron Radiation Facility, ESRF, in Grenoble. The synchrotron was operating in the uniform filling mode at a storage ring

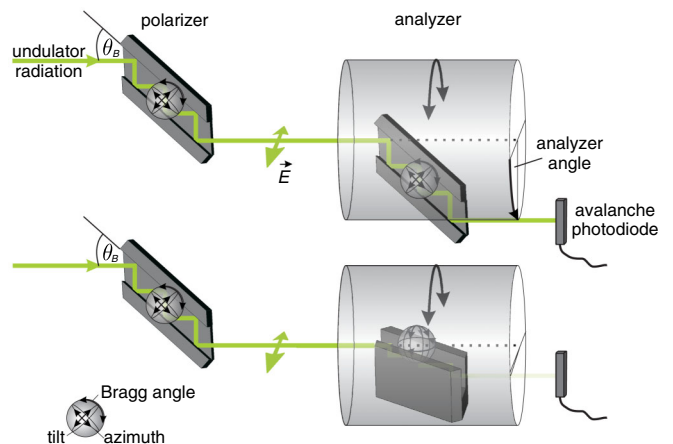


FIG. 2 (color online). Scheme of the experimental setup shown in transmission (upper part) and crossed polarizer (lower part) configuration. Also indicated are the other relevant angles besides the analyzer angle. For the polarizer, the Bragg angle  $\theta_B$  is adjusted by rotation about an axis vertical on the drawing plane. Rotation about an axis parallel to the channel affects the tilt angle and rotation about an axis perpendicular on the channel walls the azimuth.

current of less than 200 mA. The horizontal and vertical rms beam divergence was  $10.3 \mu\text{rad}$  and  $2.9 \mu\text{rad}$ , respectively. The white beam was monochromatized by a double-crystal Si (111) high-heat load monochromator which leads to an energy bandwidth smaller than 1.5 eV. In order to reduce possible higher harmonics in the beam which could excite additional multiple-beam cases, the pitch of the monochromator was slightly detuned. Before the main experiment, the energy of the high-heat load monochromator was adjusted with the help of a single silicon crystal monolith with two surfaces parallel to the lattice planes (001) and (010). As the lattice planes (001) and (010) are perpendicular to each other, the intensity of the beam reflected at both planes reaches its maximum when the energy has been adjusted such that the kinematical Bragg angle is exactly  $45.000^\circ$ . The slight change in wavelength due to diffraction leads to a small modification of the Bragg angle in the crystal. We have verified that this change does not modify the polarization purity.

Both the polarizer and analyzer are designed as six-reflection channel-cut crystals. Each channel cut was mounted on a goniometer for adjustment of the Bragg angle and circle segments stages for changing the crystal tilt as well as the crystal azimuth. The analyzer crystal was attached to an additional goniometer to rotate the crystal around the diffracted beam of the polarizer channel cut. The full-step resolutions of the goniometers and circle segments (tilt, azimuth) are 0.9 and 30 arcsec, respectively. The photon flux impinging on the polarizer was recorded by an ionization chamber. Depending on the rate, the flux behind the analyzer was detected by a photodiode or a more sensitive avalanche photodiode.

The polarization purity measurement, shown in Fig. 3, was performed by rotating the analyzer channel-cut crystal around the diffracted beam of the polarizer channel-cut crystal. In each position the rocking curve was measured and normalized to the incoming photon flux in front of the

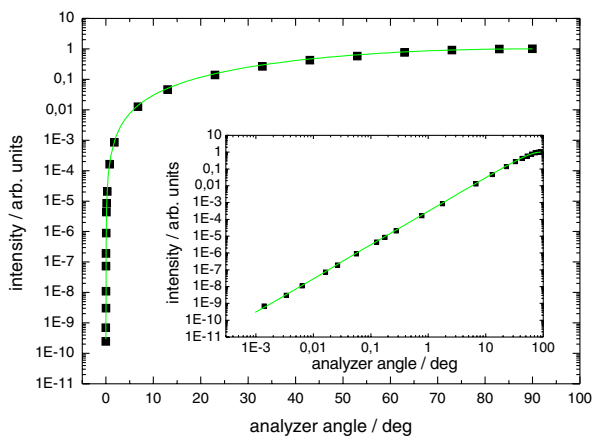


FIG. 3 (color online). Measurement of the polarization purity of an x-ray beam of energy 6.457 keV using Si(400) six-reflection channel cuts. The inset displays the data in a double-logarithmic scale.

polarizer. In the crossed position, the azimuth of the crystals was varied to obtain the best polarization purity. Every data point in the plot shows the integrated intensity of the rocking curve in the particular analyzer position normalized to the integrated intensity of the rocking curve in the passage direction (analyzer position =  $90^\circ$ ). For this measurement a pair of Si(400) channel cuts has been used at 6.457 keV photon energy. We have achieved a polarization purity of  $(2.4 \pm 0.9) \times 10^{-10}$ . At an x-ray energy of 12.914 keV, a polarization purity of  $(5.7 \pm 2.1) \times 10^{-10}$  was obtained. This is an improvement of nearly one order of magnitude for low energies and one and a half orders for the higher energies as compared to our previous results [9], where we used four-reflection channel cuts that already had improved the state of the art by about 2 orders of magnitude. The sensitivities corresponding to these purities are unique in optics and can be expected to enable novel applications.

The extreme performance of the x-ray polarimeter can be demonstrated by adapting a classical polarimetry experiment in the visible spectral range, namely the measurement of the optical activity of sucrose. In the visible, the optical activity of solutions arises from mixed electric and magnetic dipole transitions ( $E1M1$ ) between chiral molecular orbitals. In the x-ray regime, however, magnetic dipole transitions are forbidden by the  $\Delta n = 0$  selection rule. Other mixed multipole transitions like electric dipole and quadrupole transitions ( $E1E2$ ) can occur and are in fact known to be responsible for x-ray magnetic circular dichroism. However, they depend on the orientation of the molecules and, again, the optical activity vanishes for randomly orientated systems like solutions. Therefore, the optical activity of solutions that arises from inner shells can only be observed if the  $1s$  orbital mixes with valence molecular states and  $E1M1$  transitions are not forbidden anymore. For carbon compounds this was studied theoretically and first measured on methyloxirane vapor by Alagna, Turchini, and co-workers [19,20]. Achieving information on the coupling of inner-shell and valence states is a topic in several fields of science including x-ray physics with free-electron lasers and attosecond laser physics. The ability to detect chiral properties of matter with deeply penetrating x rays may also find applications in analytical chemistry, if x-ray polarimeters can be further improved. With our x-ray polarimeter, x-ray optical activity can also be observed in liquid solutions. Since the photon energy is far from absorption edges, samples are not restricted to thin liquid films or gases.

Our sample, inserted between the polarizer and analyzer, was a 13 mm long cuvette filled with a sucrose solution (with a concentration of  $\approx 400 \text{ g/l}$ ). The measurements were performed at an x-ray energy of 12.914 keV. Figure 4 shows the intensity behind the analyzer during the variation of the analyzer angle close to the crossed-polarizer position with and without the sample. Each data point is the sum of 11 measurements with an acquisition time of 5 sec. In order to reduce the influence of possible drifts, the measurements were carried out alternately with and



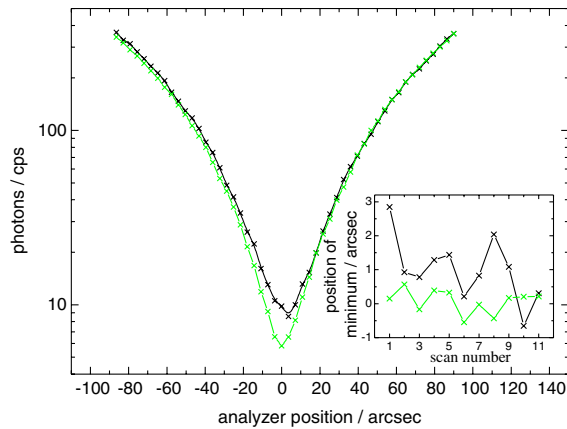


FIG. 4 (color online). X-ray polarimetry on a solution of sucrose. The shift of the position of maximum extinction (black curve) corresponds to a rotation of the polarization plane by 0.9 arcsec and an induced ellipticity  $\epsilon^2 = 2.3 \times 10^{-10}$ . The green (lower) curve displays the measurement without the sample. Each data point has been measured 11 times as illustrated in the inset.

without the sample. In addition, the absorption of radiation in the sample was measured independently.

In the inset of Fig. 4, the angular position of the minimum intensity is shown for each measurement with and without the sample. The curve without the sample shows the stability and reliability of the system. The error of about 1 arcsec is caused by noise due to the small number of photons in the area of suppression. Due to absorption, the error becomes larger when the empty cuvette is replaced by one filled with sucrose solution. The result of this experiment is a shift of the minimum in direction of both the ordinate and the abscissa. This shift can be attributed to a rotation of  $(0.9 \pm 0.5)$  arcsec of the polarization plane and an ellipticity  $\epsilon^2 = (2.3 \pm 0.9) \times 10^{-10}$ , where  $\epsilon$  is the ratio of the field strength in the  $\pi$  and  $\sigma$  direction. The rotation of the polarization can be used to infer the rotational strength  $R$  at the carbon  $K$  edge, which equals the imaginary part of the product of the electric and magnetic dipole moments: it is of the order of  $10^{-55}$  C<sup>2</sup>m<sup>3</sup>/s, which agrees well with predictions for carbon-oxygen compounds by Alagna [19].  $R$ , which is the sum of all rotational strengths at the  $K$  edge in this case, can also be estimated using the Rosenfeld equation [21] which confirms our interpretation; see the Supplemental Material [22].

In conclusion, we have improved x-ray polarimeters such that several orders of magnitude in higher polarization purities are achieved than are available in the visible spectral range. Conclusive evidence was presented that multiple beam diffraction needs to be suppressed further for further improvements. The x-ray polarimeters presented allow detection of rotations of the polarization plane down to 1 arcsec. The performance of the polarimeters was demonstrated by detecting the optical activity of sucrose which shows that inner shell orbitals are influenced by the molecular structure.

We would like to thank H. Marschner, H. Schulte-Schrepping, and D. Stachel for crystal preparation and for useful information. This work was supported by the German Science Foundation (DFG TR18) and Carl-Zeiss-Stiftung.

\*berit.marx@uni-jena.de

- [1] C. G. Barkla, *Nature (London)* **69**, 463 (1904).
- [2] H. Cole, F. W. Chambers, and C. G. Wood, *J. Appl. Phys.* **32**, 1942 (1961).
- [3] M. Hart and A. R. D. Rodrigues, *Philos. Mag. B* **40**, 149 (1979).
- [4] U. Spillmann, H. Bräuning, S. Hess, H. Beyer, Th. Stohlker, J.-Cl. Dousse, D. Protic, and T. Krings, *Rev. Sci. Instrum.* **79**, 083101 (2008).
- [5] L. Paolasini *et al.*, *J. Synchrotron Radiat.* **14**, 301 (2007).
- [6] F. de Bergevin and M. Brunel, *Acta Crystallog. Sect. A* **37**, 314 (1981).
- [7] E. E. Alp, W. Sturhahn, and T. S. Toellner, *Hyperfine Interact.* **125**, 45 (2000).
- [8] R. Röhlberger, E. Gerdau, R. Ruffer, W. Sturhahn, T. S. Toellner, A. I. Chumakov, and E. E. Alp, *Nucl. Instrum. Methods Phys. Res., Sect. A* **394**, 251 (1997).
- [9] B. Marx, I. Uschmann, S. Höfer, R. Löttsch, O. Wehrhan, E. Förster, M. Kaluza, T. Stöhlker, H. Gies, C. Detlefs, T. Roth, J. Härtwig, and G. G. Paulus, *Opt. Commun.* **284**, 915 (2011).
- [10] J. J. Klein and B. P. Nigam, *Phys. Rev.* **135**, B1279 (1964).
- [11] T. Heinzl, B. Liesfeld, K. U. Amthor, H. Schwöerer, R. Sauerbrey, and A. Wipf, *Opt. Commun.* **267**, 318 (2006).
- [12] H. Gies, J. Jaekel, and A. Ringwald, *Phys. Rev. Lett.* **97**, 140402 (2006).
- [13] R. Cameron, G. Cantatore, A. C. Melissinos, G. Ruoso, Y. Semertzidis, H. J. Halama, D. M. Lazarus, A. G. Prodell, F. Nezrick, C. Rizzo, and E. Zavattini, *Phys. Rev. D* **47**, 3707 (1993).
- [14] K. P. Heeg, H.-C. Wille, K. Schlage, T. Guryeva, D. Schumacher, I. Uschmann, K. S. Schulze, B. Marx, T. Kämpfer, G. G. Paulus, R. Röhlberger, and J. Evers, "Vacuum-assisted generation and control of atomic coherences at x-ray energies" (to be published).
- [15] T. Toellner, E. Alp, W. Sturhahn, T. Mooney, X. Zhang, M. Ando, Y. Yoda, and S. Kikuta, *Appl. Phys. Lett.* **67**, 1993 (1995).
- [16] J. DuMond, *Phys. Rev.* **52**, 872 (1937).
- [17] M. Hart, *Philos. Mag. B* **38**, 41 (1978).
- [18] J. Z. Tischler and B. W. Batterman, *Acta Crystallog. Sect. A* **42**, 510 (1986).
- [19] L. Alagna, S. Di Fonzo, T. Prospero, S. Turchini, P. Lazzeretti, M. Malagoli, R. Zanasi, C. R. Natoli, and P. J. Stephens, *Chem. Phys. Lett.* **223**, 402 (1994).
- [20] S. Turchini, N. Zema, S. Zennaro, L. Alagna, B. Stewart, R. D. Peacock, and T. Prospero, *J. Am. Chem. Soc.* **126**, 4532 (2004).
- [21] D. P. Braig and T. Thirunamachandran, *Molecular Quantum Electrodynamics* (Dover, New York, 1998).
- [22] See Supplemental Material at <http://link.aps.org/supplemental/10.1103/PhysRevLett.110.254801> for estimation of optical activity of sucrose in the x-ray range.